The FEBS Journal

FEBS PRESS science publishing by scientists

Mitotic entry upon Topo II catalytic inhibition is controlled by Chk1 and Plk1

Maria Arroyo[1], Ana Cañuelo[1], Jesús Calahorra[1], Florian D. Hastert[3], Antonio Sánchez[1], Duncan J. Clarke[2] and J. Alberto Marchal[1]

1 Departamento de Biología Experimental, Universidad de Jaén, Spain
2 Department of Genetics, Cell Biology and Development, University of Minnesota, Minneapolis, MN, USA
3 Department of Biology, Technische Universität Darmstadt, Germany

Keywords
checkpoint adaptation; Chk1; MCPH1; Plk1; topoisomerase II

Correspondence
J. A. Marchal, Departamento de Biología Experimental, Facultad de Ciencias Experimentales, Universidad de Jaén, Paraje Las Lagunillas s/n; Room B3-304, E-23071 Jaén, Spain
Tel: +34-953213361
E-mail: jamaor@ujaen.es

(Received 27 June 2019, revised 13 January 2020, accepted 3 March 2020)

doi:10.1111/febs.15280

Catalytic inhibition of topoisomerase II during G2 phase delays onset of mitosis due to the activation of the so-called decatenation checkpoint. This checkpoint is less known compared with the extensively studied G2 DNA damage checkpoint and is partially compromised in many tumor cells. We recently identified MCPH1 as a key regulator that confers cells with the capacity to adapt to the decatenation checkpoint. In the present work, we have explored the contributions of checkpoint kinase 1 (Chk1) and polo-like kinase 1 (Plk1), in order to better understand the molecular basis of decatenation checkpoint. Our results demonstrate that Chk1 function is required to sustain the G2 arrest induced by catalytic inhibition of Topo II. Interestingly, Chk1 loss of function restores adaptation in cells lacking MCPH1. Furthermore, we demonstrate that Plk1 function is required to bypass the decatenation checkpoint arrest in cells following Chk1 inhibition. Taken together, our data suggest that MCPH1 is critical to allow checkpoint adaptation by counteracting Chk1-mediated inactivation of Plk1. Importantly, we also provide evidence that MCPH1 function is not required to allow recovery from this checkpoint, which lends support to the notion that checkpoint adaptation and recovery are different mechanisms distinguished in part by specific effectors.

Introduction

G2 cell cycle checkpoints delay the onset of mitosis in response to a wide variety of genotoxic stresses. The induced arrest is necessarily reversible, allowing cells to resume progression once the damage is fully repaired [1]. In cases where the damage is too extensive or unrepairable, cells exit from the cell cycle and undergo senescence or programmed cell death [2,3]. However, an alternative less-understood cell response is checkpoint adaptation, a process where cells spontaneously bypass the checkpoint arrest despite the persistence of the damage that triggered the G2 delay [4-7]. Since cells entering mitosis with unrepaired damaged DNA are a source of genomic instability, checkpoint adaptation is considered a potential contributor to tumorigenesis and cancer resistance during genotoxic therapy. Importantly, checkpoint adaptation is conceptually different from checkpoint recovery, which refers to feedback mechanisms that allow exit from the

Abbreviations
ATM, ataxia telangiectasia mutated; ATR, ataxia telangiectasia and Rad3-related; Cdc25, cell division cycle 25A; Cdk1, cyclin-dependent kinase 1; Chk1, checkpoint kinase 1; DSBs, double-strand breaks; DT40, chicken bursal lymphoma cell line; ICRF-193, 4-[2-(3,5-Dioxo-1-piperazinyl)-1-methylpropyl]piperazine-2,6-dione; IR, ionizing radiation; LCLs, lymphoblast cell lines; MCPH1, microcephalin 1; NEB, nuclear envelope breakdown; PLCs, prophase-like cells; Plk1, polo-like kinase 1; SWI/SNF, SWItch/sucrose nonfermentable nucleosome remodeling complex.

arrest by extinguishing the checkpoint signal once the damage is dealt with to ensure cell cycle reentry [8].

The molecular basis underlying G2 checkpoint adaptation in human cells remains elusive. Our current knowledge is predominantly derived from studies of cell responses to lesions inducing double-strand breaks (DSBs) in the DNA [8]. However, the pathways conferring adaptation to other G2 checkpoints are less explored. In a recent study [9], we demonstrated that microcephalin 1 (MCPH1) function is required for bypass of the so-called 'decatenation checkpoint', a G2 pathway that delays entry into mitosis in response to catalytic inhibition of DNA topoisomerase II (Topo II; reviewed in [10]). MCPH1 is a gene mutated in primary microcephaly, which regulates a variety of processes during the cell cycle, including centrosome function, DNA repair, and chromosome dynamics (reviewed in [11]). Interestingly, cells lacking MCPH1 function became permanently arrested in G2 upon incubation with the Topo II catalytic inhibitor 4-[2-(3,5-Dioxo-1-piperazinyl)-1-methylpropyl]piperazine-2,6-dione (ICRF-193), which triggers checkpoint activation. This was surprising considering that the decatenation checkpoint is especially prone to checkpoint adaptation in many tumor cell lines, where only a transient delay is observed in G2 [9-10,12]. Moreover, this permanent G2 arrest was not reversed even after caffeine inhibition of ataxia telangiectasia and Rad3-related (ATR), the primary checkpoint effector [13]. However, MCPH1 function is dispensable for decatenation checkpoint activation. Moreover, cells lacking MCPH1 function have a normal adaptation response in the context of the G2 checkpoint that responds to etoposide-induced DNA damage [9]. These data and other evidence make it clear that the G2 DNA damage checkpoint and the decatenation checkpoint are distinct signaling pathways [12,14]

Previous studies have identified several genes whose activities are required for the activation of the G2 Topo II-dependent checkpoint. Thus, if the activity of BRCA1, ATR, WRN, MDC1, TopoII, or SMC5/6 is compromised, the decatenation checkpoint becomes inactive [12,14-17]. However, what still remains poorly understood are the signals that contribute to bypass of this checkpoint. Hence, in response to catalytic inhibition of Topo II a population of cells does not permanently arrest in G2 but rather gradually enters mitosis with catenated, unresolved chromatids after delaying transiently in G2 [9]. Interestingly, attenuation of this checkpoint has been considered by some studies to contribute to the acquisition of genetic instability in some cancer cells [18]. In the present study, we have analyzed the contribution of checkpoint kinase 1 (Chk1) and polo-like kinase 1 (Plk1) to the pathway controlling mitotic entry upon Topo II inhibition. Our data suggest that Chk1 function is required to sustain the G2 arrest in response to ICRF-193 treatment, while Plk1 function is necessary for checkpoint bypass. In this context, the activity of MCPH1 appears critical for checkpoint bypass by counteracting Chk1-mediated inactivation of Plk1.

Results

Chk1 is required for decatenation checkpoint G2 arrest and functions downstream of MCPH1 during checkpoint adaptation

In a recent study, we demonstrated that MCPH1 function is required to confer cellular adaptation to the decatenation checkpoint [9]. Thus, while caffeine-induced rapid checkpoint bypass in control cells treated with ICRF-193, MCPH1-depleted cells were unable to override the ICRF-193-induced G2 arrest under the same conditions. Importantly, the observed incapacity to bypass the G2 arrest could be alternatively explained by failed recovery from this checkpoint; that is, the incapacity to silence the checkpoint once the signal that triggers it is removed. In order to answer this question, we analyzed cell cycle progression after release from prolonged incubation with ICRF-193 in HeLa H2B/Red1 cells as described previously [9]. MCPH1 depletion was achieved by transfection with validated siRNAs oligos which knocked-down the levels of this protein efficiently (Fig. 1B [9]). Transfection with siRNAs was coupled with cell synchronization at G1/S using excess thymidine, and cell cycle dynamics were monitored by fluorescent live-cell microscopy upon release from ICRF-193 incubation (experimental outline in Fig. 1A). As depicted in Fig. 1C, MCPH1-siRNA-treated cells were able to resume cell cycle progression and entered mitosis after release from the prolonged incubation with ICRF-193 although with a slight delay compared with control cells. Moreover, caffeine addition during release from ICRF-193 incubation did not interfere with the recovery capacity of MCPH1-depleted cells and accelerated entry into mitosis to the same degree as in control cells (Fig. 1D). The ablation of the recovery delay in MCPH1-depleted cells upon caffeine incubation agrees with previous evidences that demonstrated a similar acceleration in the rate of mitotic entry of MCPH1-depleted cells by caffeine during an otherwise unperturbed cell cycle [9]. In conclusion, our data underline that MCPH1 is dispensable for efficient exit from the G2 checkpoint once decatenation is achieved. The data

therefore support the hypothesis that MCPH1 function is required to confer adaptation to the decatenation checkpoint, rather than being required for checkpoint exit/recovery.

To gain further insight into the signaling pathway that controls adaptation to this checkpoint, we examined the potential role of Chk1 kinase. Chk1 is a key element of the ATR signaling pathway, but its contribution to the decatenation checkpoint remains controversial [13,19]. Previous studies have reported that MCPH1 regulates centrosomal Chk1 function during unperturbed cell cycle progression and upon activation of the DNA damage response [20,21]. Considering these molecular links between MCPH1 and Chk1, we examined if active Chk1 is required to sustain the permanent G2 arrest that is triggered in cells lacking MCPH1 function and treated with the Topo II inhibitor ICRF-193. To achieve this, we employed HeLa H2B/Red1 cells depleted of Chk1—and/or MCPH1—by RNAi as explained above (see Fig. 1F). ICRF-193 was added 6 h after release from the second thymidine block in order to inhibit Topo II at G2 phase (experimental outline in Fig. 1E). As presented in Fig. 1G, two opposite cell cycle dynamics were observed. Control cells as well as cells depleted of MCPH1 remained arrested in G2 after decatenation checkpoint activation. In both cases, adaptation was observed in a minor fraction of the cells, and this occurred earlier in control cells than MCPH1-depleted cells, in line with previous reports [9]. However, in cells depleted of Chk1 the ICRF-193-induced G2 arrest was bypassed immediately; the cells rapidly entered in mitosis. Strikingly, checkpoint bypass was also observed in cells depleted of both Chk1 and MCPH1 functions (Fig. 1G). This observation suggests that Chk1 function is required for the G2 arrest triggered by ICRF-193 and acts downstream of MCPH1 in the pathway that confers adaptation to this checkpoint. When the same experiment was repeated under unperturbed conditions, that is, in the absence of ICRF-193, cell cycle progression followed similar dynamics in all cases (Fig. 1H), which confirms that the G2 arrest was a consequence of decatenation checkpoint activation. Only a slight increase in the rate of mitosis onset was found in cells lacking Chk1 function—alone or combined with MCPH1 depletion. Interestingly, premature chromosome condensation at G2, a hallmark of MCPH1 deficiency [22,23], was also recapitulated in cells lacking both MCPH1 and Chk1 function during unperturbed cell cycle progression (Fig. 1I). This result suggests that Chk1 activity does not contribute to the altered chromosome condensation dynamics characteristic of MCPH1-depleted cells.

We next analyzed the impact of Chk1 inhibition on the cell cycle dynamics of HeLa H2B/Red1 cells once the decatenation checkpoint arrest is activated. To address this, we made use of UCN01, a well-characterized Chk1 inhibitor [24], which was added 2 h after ICRF-193 to allow decatenation checkpoint activation before Chk1 was inhibited. Live-cell imaging was started immediately afterwards (experimental outline in Fig. 2A). As shown in Fig. 2B,C, UCN01 addition induced a massive entrance into mitosis in both control and MCPH1-depleted cells treated with ICRF-193. For all these cells, mitosis occurred aberrantly, with chromosome segregation being aborted due to the lack of decatenation (Fig. 2F). Such aberrant mitotic exit was similarly observed in MCPH1 siRNA-treated cells from Fig. 2C that bypassed the decatenation checkpoint arrest. By contrast, control- and MCPH1-siRNA cells incubated only with UCN01 completed mitosis successfully (Fig. 2G). Importantly, when these experiments were repeated using CHIR-124, another chemical inhibitor of Chk1, the same results were obtained (Fig. 2D,E). Therefore, the incapacity of MCPH1-depleted cells to bypass the decatenation checkpoint arrest is restored after Chk1 inactivation.

Next, we assayed whether Chk1 activity was also required for efficient decatenation checkpoint activation in another cellular model, lymphoblastoid cells. In order to do so, we made use of log-phase cultures from one control and one MCPH1 patient and we assayed the dynamics of mitotic entry after incubation with ICRF-193, UCN01 or both during 4 and 7 h of treatment in the presence of nocodazole. The rate of mitotic accumulation was determined by flow cytometry using a mitotic marker (Histone H3PS10). As depicted in Fig. 2H, UCN01 incubation bypassed the G2 arrest imposed by ICRF-193 in both control and MCPH1 patient cells. Therefore, Chk1 activity is also required in human lymphoblastoid cells for the checkpoint arrest induced by Topo II catalytic inhibition. Moreover, the incapability to override the decatenation checkpoint arrest described previously in MCPH1 patient cells [9] was rescued by Chk1 inhibition. Single incubation with UCN01 slightly accelerates the rate of mitotic entry during the first 4 h of incubation in both control and patient cells, in line with our results in HeLa H2B/Red1 cells. By contrast, single incubation with ICRF-193 blocked mitotic entry during the time course of the experiment in both cases (Fig. 2H). When we analyzed chromosome morphology in cells treated with ICRF-193 and UCN01, we observed a high frequency of mitotic cells (more than 90%) with uncondensed and disorganized chromosomes (Fig. 2I). These alterations, observed to an equal degree in control and MCPH1 patient cells, are the expected outcome

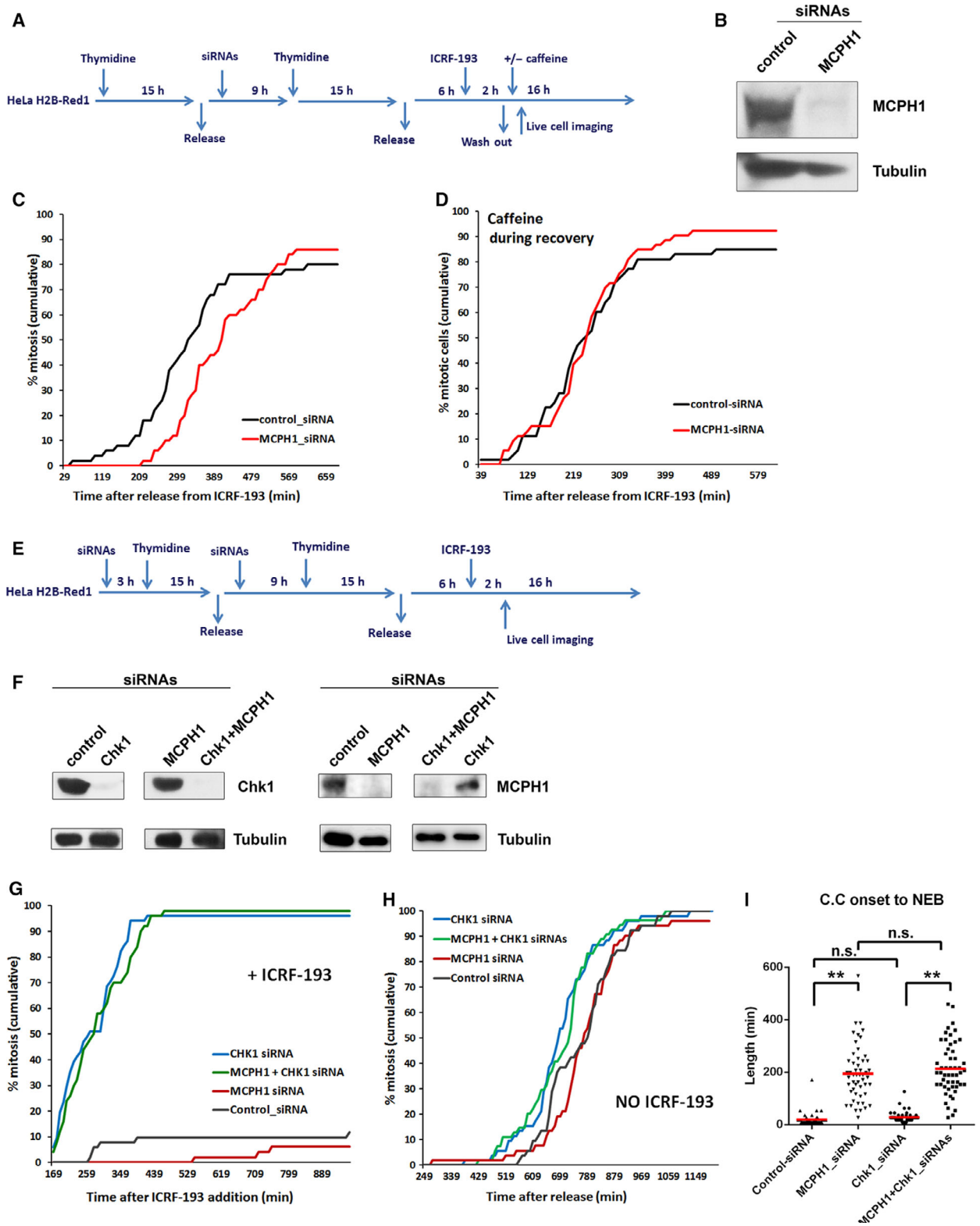

after bypass of the decatenation checkpoint and progression into mitosis without Topo II function [25,26]. However, single incubation with UCN01 did not alter chromosome structure in control cells nor in patient cells. In the case of MCPH1 patient cells, chromosomes retained the structural problems originally described as

Fig. 1. MCPH1-depleted cells are able to recover from the decatenation checkpoint arrest and capable of bypass this G2 arrest when Chk1 is simultaneously depleted by RNAi. (A) Description of the experimental procedure performed in HeLa cells stably expressing fluorescent histone H2B fused to Red1. Cells were synchronized at the G1/S border by double thymidine block. MCPH1 depletion was achieved by transfection with siRNAs duplexes during the release from the first thymidine block. ICRF-193 (7 μM) was added 6 h after release from the second thymidine block to coincide with the occurrence of PLCs during G2 in the siRNA-treated cells [47]. Time-lapse phase-contrast and fluorescent images were collected immediately after release from ICRF-193 incubation (2 h) with a Leica TCS SP5 microscope. Images were stacked and processed using IMAGEJ software. Timing data were obtained after visual inspection of mitosis onset, revealed by NEB, of 50 cells. (B) Immunoblots analyses of MCPH1 and alpha-tubulin (loading control) levels in HeLa H2B-Red1 cells treated as explained in A. (C) Cumulative frequency chart showing the timing (in minutes) of mitosis onset, revealed by NEB, during recovery from ICRF-193 incubation in HeLa H2B-Red1 cells monitored as explained in A. (D) Same recovery analyses as in 1C but with caffeine present in the medium, which was added immediately after release from ICRF-193. (E) Description of the experimental procedure. Briefly, cells were treated as in (A), but two rounds of siRNAs transfection were used this time to assure double knockdowns. (F) Immunoblots analysis of Chk1, MCPH1, and alpha-tubulin (loading control) levels in HeLa H2B-Red1 cells treated as explained in (E). (G) Cumulative frequency chart showing the timing (in minutes) of mitosis onset, revealed by NEB, after ICRF-1933 addition in HeLa H2B-Red1 cells monitored as described in (E). (H) Same analyses as in (G) but in absence of ICRF-193 treatment. Time after release from the second thymidine block is shown. (I) Box plots showing the time that chromosome condensation remained visible in cells from (D) before NEB. The red line indicates the mean value. C.C., chromosome condensation. At least 50 cells were analyzed in each case. Statistical comparisons for the mean and median data were done by Student's *t* test and Wilcoxon (W) test, respectively. $^{**}P < 0.01$; N.S. not significant.

wavy hypercondensed chromatids and resolved centromeres (Fig. 2I) [23]. In summary, our analyses clearly indicate that (a) Chk1 function is required to sustain the ICRF-193-induced G2 arrest in human cells, and (b) Chk1 loss of function restores adaptation capacity of MCPH1-depleted cells. Therefore, Chk1 inactivation appears to be the target of the MCPH1-mediated pathway triggering decatenation checkpoint adaptation.

Plk1 function is required to bypass the checkpoint arrest induced by ICRF-193 in both control and MCPH1-depleted cells

Previous studies have shown that cells treated with ICRF-193 displayed a significant although not complete inhibition of Plk1 activity, while overexpression of a constitutively active Plk1 variant abolished the decatenation checkpoint response [14,27]. These data suggest that ICRF-193-meditated G2 arrest requires inhibition of Plk1 activity, but how its function is counteracted by other modulators of this pathway is still not well understood. Considering these data, we hypothesized that Plk1 activity might be an essential factor for bypass of the decatenation checkpoint. We therefore sought to compare the activation and adaptation kinetics of the decatenation checkpoint in cells lacking Plk1 function, and the possible impact of MCPH1. To address this, we made use of synchronized HeLa H2B/Red1 cells depleted of Plk1 by RNAi either alone or combined with MCPH1. ICRF-193 was added at 7 h after release from the second thymidine block, while solvent (DMSO) was added to parallel control samples to monitor cell cycle progression in unperturbed conditions (Fig. 3A,B). Our analyses first revealed that cells depleted of either Plk1, MCPH1 or both remain permanently arrested in G2 upon ICRF-193 incubation (Fig. 3C,E). However, these cells were able to accumulate in mitosis upon release into normal medium, which confirms that the observed G2 arrest was a consequence of decatenation checkpoint activation (Fig. 3C,E). We next repeated the analysis, but we attempted to bypass the decatenation checkpoint arrest with caffeine, which was added 2 h after the ICRF-193 or solvent addition (experimental outline in Fig. 3A). As depicted in Fig. 3D,F, caffeine addition induced rapid entrance into mitosis in cells depleted of either Plk1, MCPH1, or both when released into normal medium. However, upon release into ICRF-193 no immediate override of the G2 arrest was observed for the same cells. Following several hours, some cells were able to bypass the arrest; however, at least 60% remained permanently arrested in the presence of ICRF-193 and caffeine (Fig. 3D,F). Importantly, similar results were observed when we repeated these experiments using a different siRNA oligo against Plk1 (Fig. 3G–I). Therefore, the ability of caffeine to bypass the G2 decatenation checkpoint that we and others previously described [9,15] was strongly perturbed if Plk1 function was depleted by RNAi.

To confirm these findings, we repeated these experiments using an alternative method to inhibit Plk1 function. This was achieved by using a well-characterized inhibitor, BI2536 [28,29], which was added 2 h after ICRF-193 addition either alone or combined with caffeine (experimental setup in Fig. 4A). Our analyses first demonstrated that the G2 arrest observed for control cells upon ICRF-193 incubation was not bypassed after caffeine incubation if Plk1 function was inhibited by

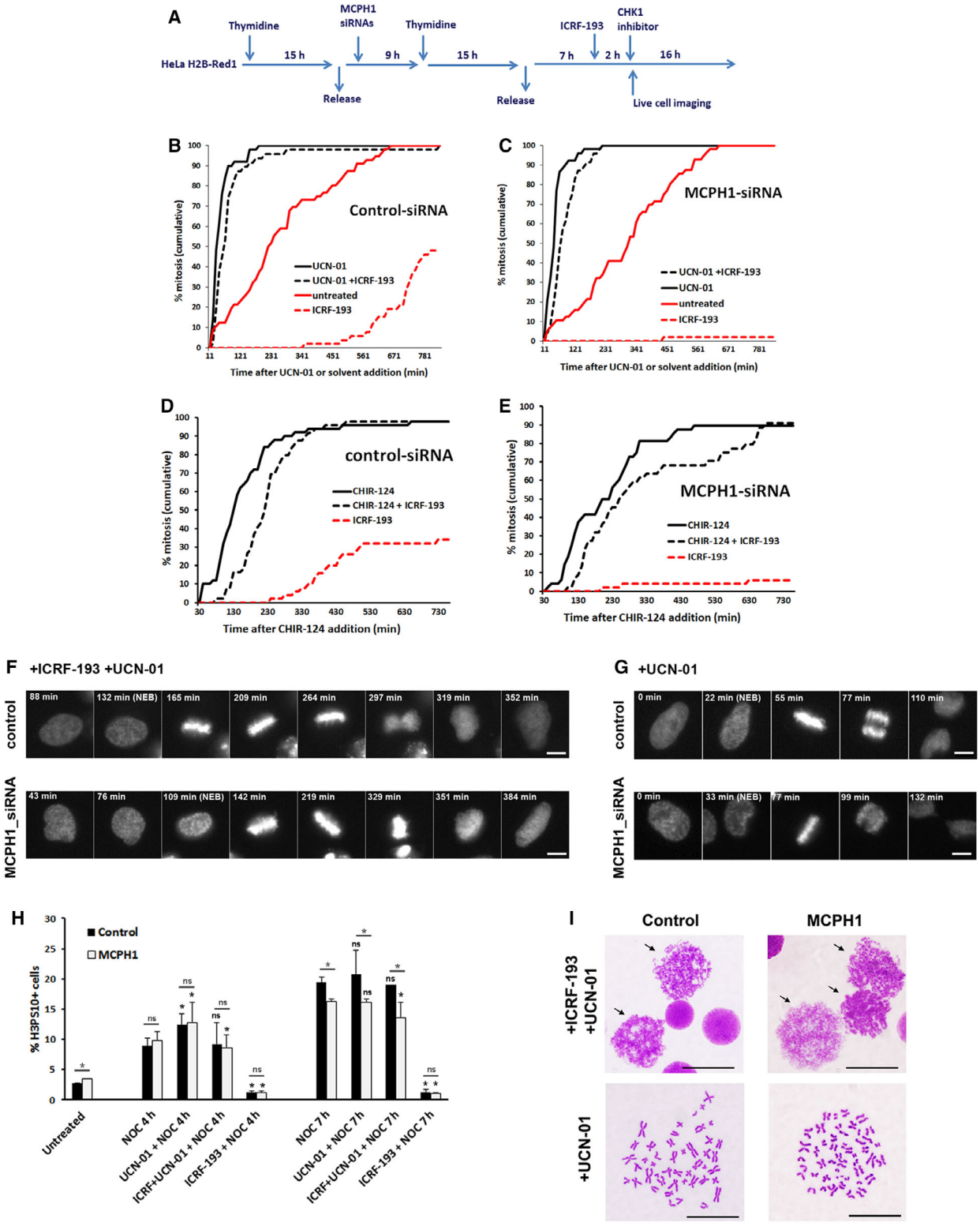

BI2536 (Fig. 4B,F). When the same analyses were repeated in cells depleted of MCPH1 by RNAi, a similar response was observed (Fig. 4C,F). The G2 arrest in the presence of BI2536 was more robust compared to the observed arrest in Plk1-siRNA-treated cells. Interestingly, MCPH1 depletion reinforced the incapacity of

Fig. 2. Chk1 inactivation is the target of the MCPH1-mediated pathway triggering decatenation checkpoint adaptation. (A) Description of the experimental procedure performed. HeLa H2B-Red1 cells were synchronized at the G1/S border by double thymidine block. MCPH1 depletion was achieved by transfection with siRNAs duplexes during the release from the first thymidine block. ICRF-193 (7 μM) or solvent (DMSO) was added 7 h after release from the second thymidine block to coincide with the occurrence of PLCs during G2 in the siRNA-treated cells [47]. Chk1 inhibitor was added 2 h afterward. Time-lapse phase-contrast and fluorescent images were collected immediately after UCN01 addition with a Leica TCS SP5 microscope. Images were stacked and processed using IMAGEJ software. Timing data were obtained after visual inspection of mitosis onset, revealed by NEB, of 50 cells. (B, C) Cumulative frequency chart showing the timing (in minutes) of mitosis onset, revealed by NEB, of control cells (B) and MCPH1-depleted cells (C) after the indicated treatments as explained in (A). Time after UCN01 or solvent addition is shown. (D, E) Cumulative frequency chart showing the timing of mitosis onset of control cells (D) and MCPH1-depleted cells (E) after the indicated treatments as explained in (A). Time after CHIR-124 or solvent addition is shown. (F) Selected frames showing the mitotic progression of representative control and MCPH1-depleted HeLa cells treated with UCN01 and ICRF-193. Time from UCN01 addition is indicated in minutes. Note that cells end mitosis aberrantly as chromosome segregation is prevented. Scale bars, 10 μM. (G) Selected frames showing the mitotic progression of representative control and MCPH1-depleted HeLa cells treated only with UCN01. Time from UCN01 addition is indicated in minutes. In this case, cells progress normally through mitosis. Scale bars, 10 μM. (H) Frequency of histone H3PS10-positive cells in control and MCPH1 patient lymphoblastoid cells, determined by flow cytometry, after incubation with nocodazole alone or combined with UCN01, ICRF-193, or both for the indicated time points. Mean and range (bars) data from two independent experiments are presented. For each time point, pooled data for each treatment were compared independently in control and patient cells by chi-squared test of independence to nocodazole-treated cells. Furthermore, for each treatment and time point, control and patient data were pairwise compared by chi-squared test of independence (underlined). ns, nonsignificant. $*P < 0.01$. (I) Representative images from cytogenetic preparations of control and MCPH1 patient cells treated simultaneously with ICRF-193 and UCN01. Arrows point to mitotic cells showing entangled and disorganized chromosomes, typical of cells treated with Topo II inhibitors, which were equally observed in both samples. In comparison, cells treated only with UCN01 show normal mitotic chromosomes. Scale bars, 5 μM.

cells lacking Plk1 function to bypass the arrest (compare the kinetics of BI2536-treated cells from Fig. 4B,C), which suggests that both proteins have synergistic effects on the mechanism triggering decatenation checkpoint bypass. In order to rule out that the observed G2 arrest was a direct consequence of the incubation with BI2536 itself, we performed similar analyses in synchronized cells treated only with BI2536 upon release into normal medium. Our data clearly demonstrate that under non-DNA-damaging conditions, Plk1 inhibition delays but does not block the onset of mitosis in both control (Fig. 4D) and MCPH1-siRNA-treated cells (Fig. 4E). As expected from cells lacking Plk1 function, the cells were further unable to complete chromosome alignment and segregation (Fig. 4G), a hallmark of the 'Polo' phenotype [28,30].

We next analyzed if inhibition of Plk1 function by BI2536 impairs the capacity to bypass the decatenation checkpoint in another cellular model, lymphoblastoid cells. To address this, we made use of log-phase lymphoblast cultures from control and MCPH1 patient cells and assayed the dynamics of mitotic entry after prolonged incubation with BI2536 alone or combined with ICRF-193, caffeine, or both. Our data first demonstrated that inhibition of Plk1 by BI2536 slowed down the accumulation of mitotic cells in both control and MCPH1 patient cells, in comparison with the progressive accumulation observed when only nocodazole was added (Fig. 5A,C). In parallel with reduced mitotic entry, the fraction of G2 cells increased during prolonged incubation with BI2536 and nocodazole (data not shown). Therefore, in accordance with our previous findings in HeLa cells, inhibition of Plk1 by BI2536 delays but does not block entry into mitosis in control and MCPH1 patient lymphoblast cells, as was observed upon single incubation with ICRF-193. Our results are in accordance with previous studies which demonstrated that mitotic entry is delayed but not blocked following Plk1 inhibition [31,32]. Moreover, to gain more information about the efficiency of Plk1 inhibition in lymphoblastoid cells we analyzed chromosome morphology. As depicted in Fig. 5E, chromosomes from both control and patient cells appeared hypercondensed and the sister chromatids retained cohesion after prolonged incubation with B12536 and nocodazole. However, in cells treated only with nocodazole chromosomes were less compacted and the cohesion between chromatids was removed. These results are in agreement with previous descriptions of the impact of Plk1 inhibition on mitotic chromosome organization [29].

When ICRF-193 was added in combination with BI2536, mitotic cells did not accumulate either in control cells or in patient cells during the time course of the experiment (Fig. 5B,D). In parallel, the frequency of G2 cells increased over time (data not shown). Caffeine addition did not have any effect on the mitotic rate of control and patient cells treated with ICRF-193 and BI2536 (Fig. 5B,D). As predicted [9], when caffeine was added to cells treated only with ICRF-193 mitotic cells accumulated over time in control but not in MCPH1 patient cells. In agreement with our previous observation in HeLa H2B/Red1 cells, these results demonstrate

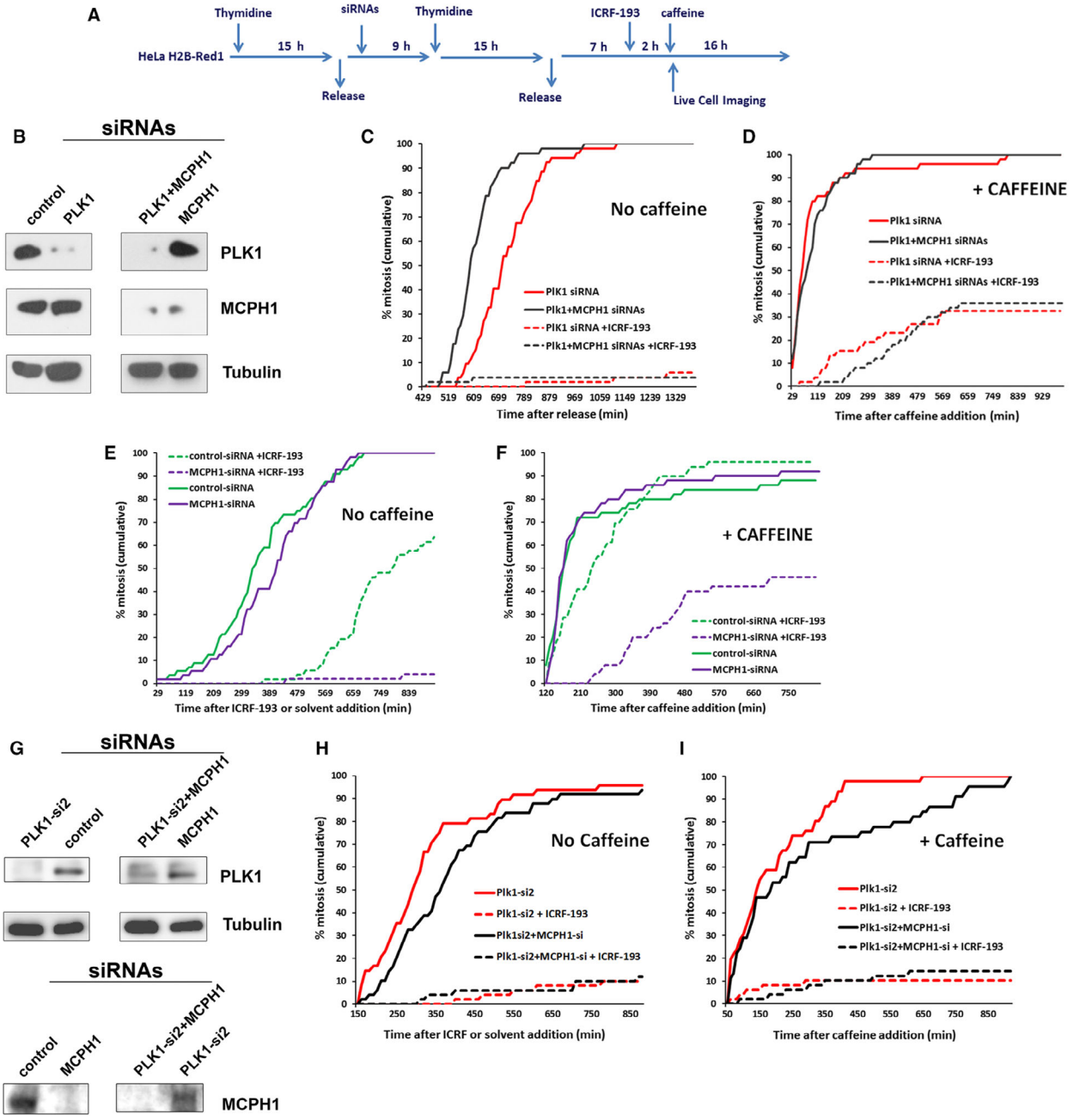

Fig. 3. The ability of caffeine to bypass the G2 decatenation checkpoint is strongly perturbed if Plk1 function is depleted by RNAi. (A) Description of the experimental procedure performed. HeLa H2B-Red1 cells were synchronized at the G1/S border by double thymidine block. MCPH1 depletion and/or Plk1 depletion were achieved by transfection with siRNAs duplexes during the release from the first thymidine block. ICRF-193 (7 μM) or solvent (DMSO) was added 7 h after release from the second thymidine block, while caffeine or solvent (medium) was added 2 h afterward. Time-lapse phase-contrast and fluorescent images were collected immediately after UCN01 with a Leica TCS SP5 microscope. Images were stacked and processed using IMAGEJ software. Timing data were obtained after visual inspection of mitosis onset, revealed by NEB, of 50 cells. (B) Immunoblot analysis of Plk1, MCPH1, and alpha-tubulin (loading control) levels in HeLa H2B-Red1 cells transfected with the indicated siRNAs as explained in (A). (C–F) Cumulative frequency chart showing the timing (in minutes) of mitosis onset, revealed by NEB, of HeLa H2B-Red1 cells after the corresponding treatments in the absence (C, E) or presence of caffeine (D, F) as explained in (A). (G) Immunoblot analysis of Plk1, MCPH1, and alpha-tubulin (loading control) levels in HeLa H2B-Red1 cells transfected with the indicated siRNAs. (H, I) Same analyses as in (C) and (D) but using a different siRNA oligo against Plk1.

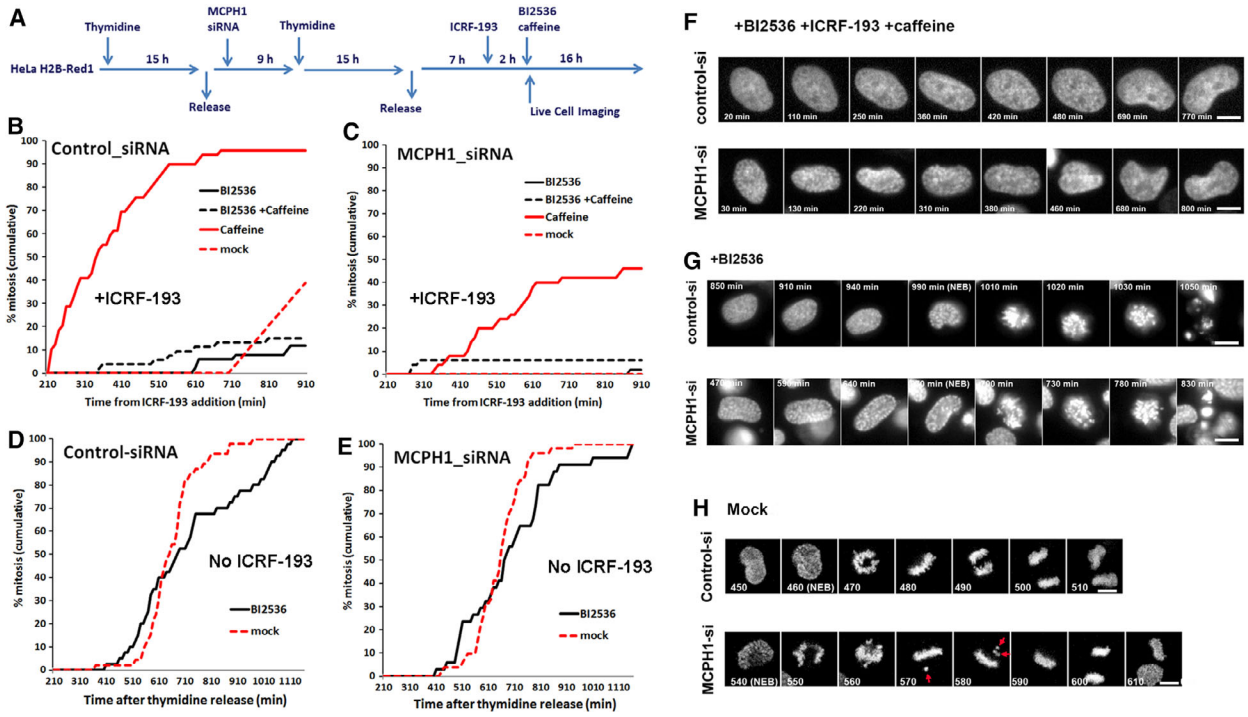

Fig. 4. The ability of caffeine to bypass the G2 decatenation checkpoint is strongly perturbed if Plk1 function is blocked by chemical inhibitors. (A) Description of the experimental procedure performed. HeLa H2B-Red1 cells were synchronized at the G1/S border by double thymidine block. MCPH1 depletion was achieved by transfection with siRNAs duplexes during the release from the first thymidine block. ICRF-193 (7 μM) was added 7 h after release from the second thymidine block. BI2536 and/or caffeine were added 2 h later, and time-lapse phase-contrast and fluorescent images were collected immediately afterward with a Leica TCS SP5 microscope. Images were stacked and processed using IMAGEJ software. Timing data were obtained after visual inspection of mitosis onset, revealed by NEB, of 50 cells. (B, C) Cumulative frequency chart showing the timing (in minutes) of mitosis onset, revealed by NEB, of control (B) and MCPH1-depleted (C) HeLa H2B-Red1 cells after the corresponding treatments in the presence of ICRF-193. Time after ICRF-193 addition is shown. (D, E) Cumulative frequency chart showing the timing (in minutes) of control (D) and MCPH1-depleted (E) HeLa H2B-Red1 cells treated with solvent or BI2536 upon release from the second thymidine block. Time after release from the second thymidine block is shown. (F) Selected frames showing the condensation dynamics of control and MCPH1-siRNA-treated HeLa cells while arrested in G2 by simultaneous ICRF-193, BI2536, and caffeine incubation. Time from caffeine addition is indicated in minutes. Scale bars, 10 μM. (G, H) Selected frames showing the mitotic progression of representative control and MCPH1-depleted HeLa cells treated with BI2536 (G) or untreated (H). Time from the second thymidine release is shown. Note that in the first case cells were unable to perform chromosome alignment and segregation as a consequence of Plk1 inhibition. However, in the absence of the Plk1 inhibitor cells completed mitosis successfully. Note that chromosome alignment at prometaphase is delayed in the absence of MCPH1 function, in agreement with previous reports (delayed chromosomes indicated by red arrows). Scale bars, 10 μM.

that the ability of caffeine to induce decatenation checkpoint bypass is prevented if Plk1 function is also inhibited in human lymphoblastoid cells. Taken together, our data clearly indicate that Plk1 function is required to bypass the G2 arrest induced by catalytic inhibition of Topo II in human cells.

Wee1 does not contribute to the MCPH1-dependent pathway controlling decatenation checkpoint adaptation

Finally, we were interested in determining the contribution of Wee1 to the decatenation checkpoint, which remained unknown. Wee1 is a kinase that selectively phosphorylates the Y15 residue of cyclin-dependent kinase 1 (Cdk1) and promotes its inactivation. This inhibitory function is antagonized by cell division cycle 25A (Cdc25) phosphatases. As cells progress through G2, the balance of Wee1 and Cdc25 determines the timing of Cdk1 full activation, and consequently, mitosis onset [33]. We first examined if inactivation of Wee1 alters the duration of the G2 arrest induced by ICRF-193 in HeLa H2B/Red1 cells transfected with control- or MCPH1-siRNAs. To this end, we made use of MK1775, a potent small-molecule inhibitor that ablates Wee1 function [34]. MK1775 was added 2 h after ICRF-193 or mock addition (experimental outline in Fig. 6A). As shown in Fig. 6B, MK1775

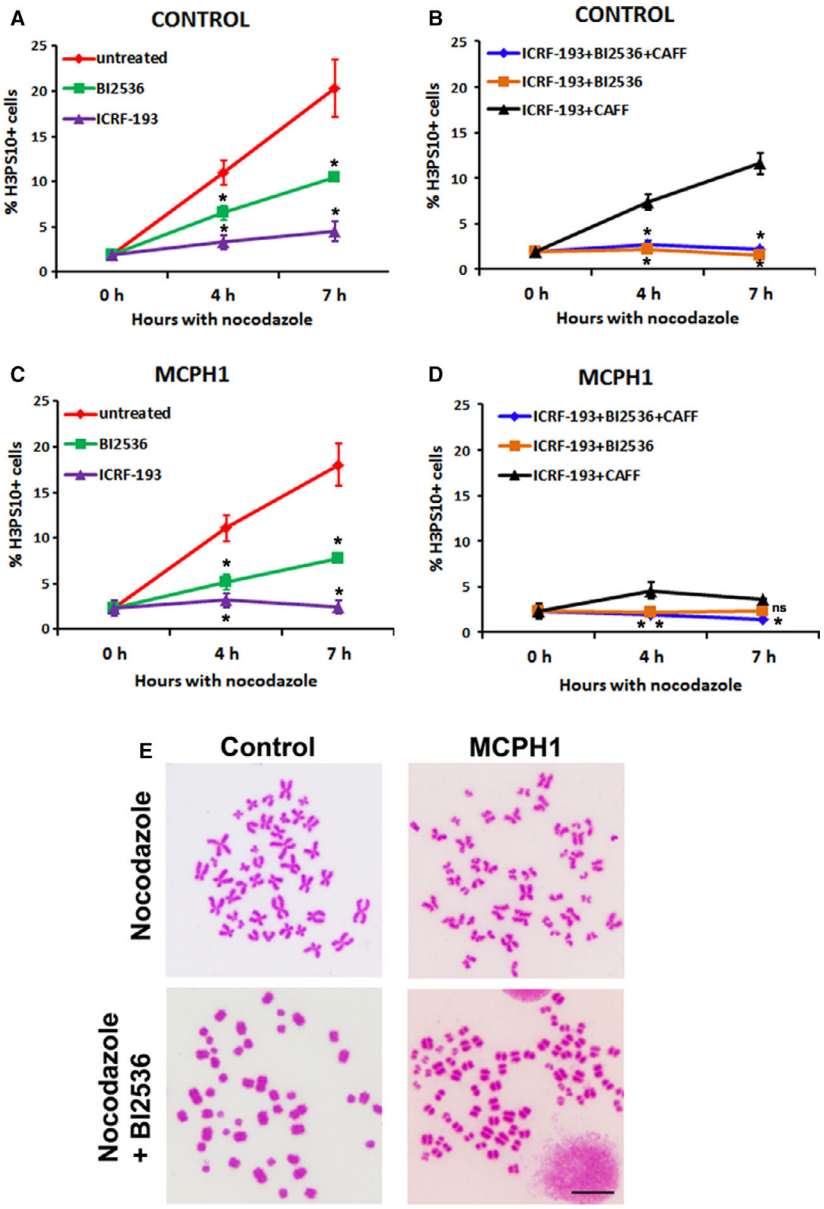

Fig. 5. Plk1 function is required for caffeine to induce decatenation checkpoint bypass in human lymphoblastoid cells. (A–D) Frequency of histone H3PS10-positive cells in control (A, B) and MCPH1 patient (C, D) lymphoblastoid cells, determined by flow cytometry, after 4 or 7 h of incubation with nocodazole alone or in combination with the indicated inhibitors. Mean and range (bars) data from two independent experiments are presented. For each time point from A and C, pooled data for each treatment were compared independently by chi-squared test of independence to nocodazole-treated cells. For each time point from B and D, pooled data were similarly compared to cells treated with ICRF and caffeine. ns, nonsignificant. $*P < 0.01$. (E) Representative images from cytogenetic preparations of control and MCPH1 patient cells treated simultaneously with nocodazole alone or combined with BI2536. Scale bars, 5 μM.

addition induced a massive entrance into mitosis in control cells treated with ICRF-193. However, in MCPH1-depleted cells only a partial checkpoint bypass was observed under the same conditions and nearly 60% of cells remained arrested in G2 at the end of the analyses (Fig. 6B). To rule out the possibility that the incapacity of those MCPH1-depleted cells to override the ICRF-induced G2 arrest was a direct consequence of the incubation with MK1775 itself, we performed in parallel similar analyses in cells released into normal medium without ICRF-193. Our data clearly demonstrate that MCPH1-depleted cells accumulate rapidly in mitosis when Wee1 is inhibited by MK1775, following similar dynamics to control cells (Fig. 6B). Acceleration of mitotic entry has also been described in other cell types upon Wee1 inhibition [34,35]. These results suggest that Wee1 inhibition does not abrogate the decatenation checkpoint arrest in cells lacking MCPH1 function.

As Wee1 inactivation is controlled by Plk1 [36,37], we next analyzed if Wee1 inhibition alleviates the decatenation checkpoint arrest in cells where Plk1 function was abolished. To achieve this, we repeated the same experiments described above but in the presence of the Plk1 inhibitor BI2536 (Fig. 6A). As presented in Fig. 6C, upon ICRF-193 treatment both control and MCPH1-depleted cells remained permanently arrested in G2 when simultaneously incubated

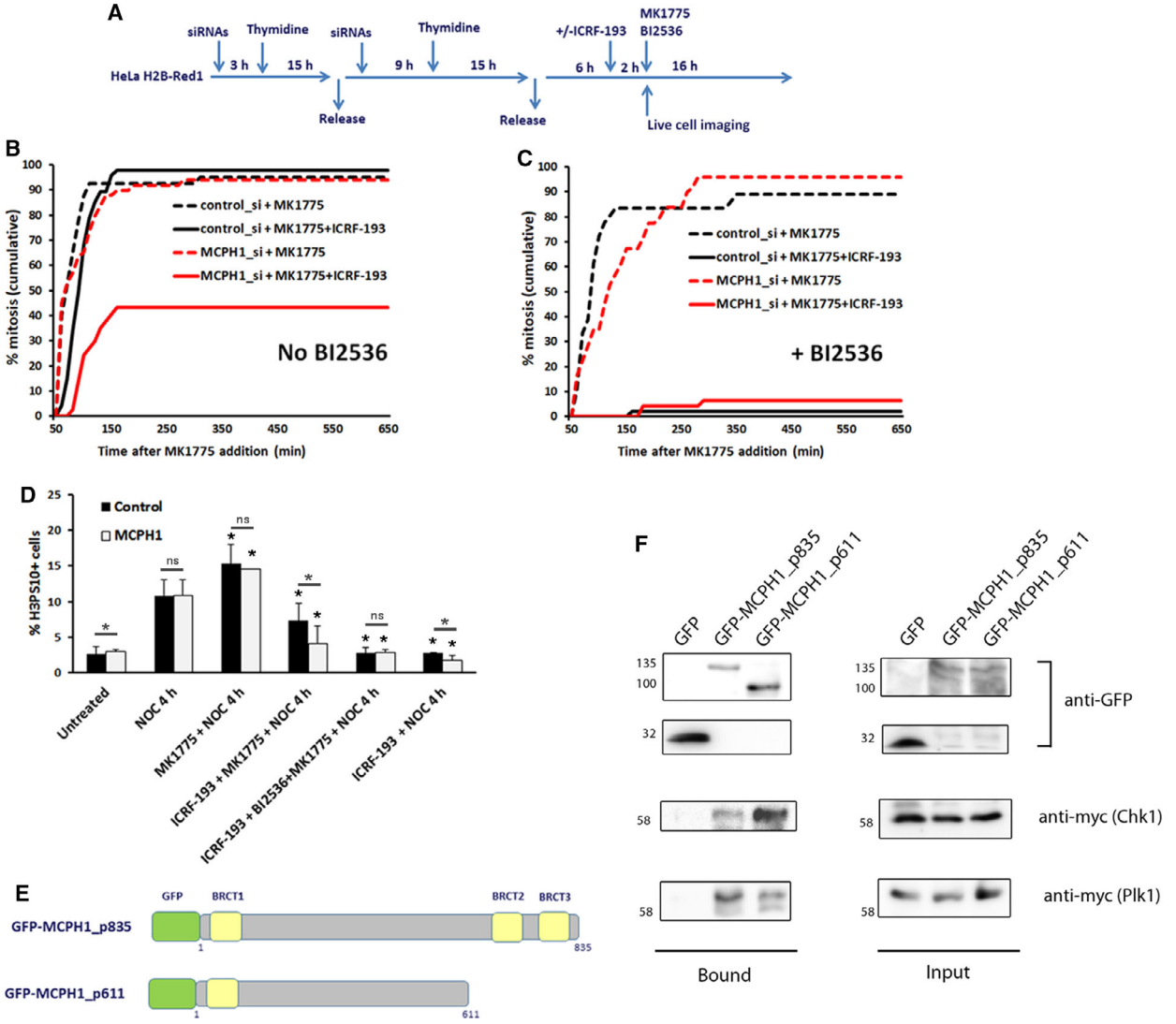

Fig. 6. Wee1 does not contribute to the MCPH1-dependent pathway controlling decatenation checkpoint adaptation. (A) Description of the experimental procedure performed. HeLa H2B-Red1 cells were synchronized at the G1/S border by double thymidine block. MCPH1 depletion was achieved by transfection with siRNAs duplexes during the release from the first thymidine block. ICRF-193 (7 μM) or solvent (DMSO) was added 6 h after release from the second thymidine block. MK1775 alone or in combination with BI2536 were added 2 h afterward, and time-lapse phase-contrast and fluorescent images were collected immediately after MK1775 addition with a Leica TCS SP5 microscope. Images were stacked and processed using IMAGEJ software. Timing data were obtained after visual inspection of mitosis onset, revealed by NEB, of 50 cells. (B, C) Cumulative frequency chart showing the timing (in minutes) of mitosis onset, revealed by NEB, of HeLa H2B-Red1 cells after the corresponding treatments in the absence (B) or presence of BI2536 (C) as explained in Fig. 3B. (D) Frequency of histone H3PS10-positive cells in control and MCPH1 patient lymphoblastoid cells, determined by flow cytometry, after 4 h of incubation with nocodazole alone or combined with MK1775, ICRF-193, and BI2536 as indicated. Mean and range (bars) data from two independent experiments are presented. For each time point, pooled data for each treatment were compared independently in control and patient cells by chi-squared test of independence to nocodazole-treated cells. Furthermore, for each treatment and time point, control and patient data were pairwise compared by chi-squared test of independence (underlined). ns, nonsignificant. $*P < 0.01$. (E) Schematic diagram showing the domain structure and size of the MCPH1 constructs employed in the pull-down analyses of protein interactions. (F) Pull-down analyses showing the *in vitro* interaction of MCPH1 with Chk1 and Plk1. GFP alone or GFP-tagged MCPH1 constructs were transfected into HEK293 cells for 48 h before purification and incubation with either myc-Chk1 or myc-Plk1 cell extracts obtained from transfected HEK293 cells. Samples were finally analyzed by western blotting using anti-myc and anti-GFP antibodies. Blots representative of two independent biological replicates are presented.

with MK1775 and BI2536. However, when released into normal medium these cells were able to accumulate into mitosis under the same conditions, which confirms that the permanent G2 arrest was a direct consequence of the decatenation checkpoint activation. These results indicate that in cells where Plk1 function is inhibited Wee1 inhibition does not abrogate the permanent G2 arrest triggered by ICRF-193. Furthermore, this response remains unaltered independently of the presence of functional MCPH1.

We also asked if comparable results are observed in lymphoblastoid cells treated under similar conditions. To achieve this, we determined the frequency of mitotic cells by FACS analysis after prolonged incubation with MK1775 either alone or combined with ICRF-193 and/or BI2536 in the presence of nocodazole (Fig. 6D). Our results first revealed that single incubation with MK1775 accelerates the rate of mitosis onset similarly in control and MCPH1 patient cells, as previously observed in HeLa cells. However, when combined with ICRF-193 it produced only partial abrogation of the ICRF-193-induced G2 arrest in control cells, while in MCPH1 patient cells, the G2 arrest remained nearly intact, with only a very minor increase in the frequency of mitotic cells observed under these conditions. When MK1775 was combined with BI2536 in the presence of ICRF-193, no mitotic accumulation neither was observed in control nor in patient cells (Fig. 6D). This result is similar to the previous data observed in HeLa cells and confirms that Wee1 inhibition does not abrogate the permanent G2 arrest triggered by ICRF-193 in cells where Plk1 function is inhibited. Therefore, our results allow us to conclude that Wee1 does not act downstream of Plk1 and MCPH1 in the central pathway that controls adaptation to the decatenation checkpoint. On the other hand, Wee1 activity could restrain spontaneous adaptation to the decatenation checkpoint through an independent secondary pathway. The increased capacity of MK1775 to abrogate the ICRF-193-induced G2 arrest in HeLa cells compared with lymphoblasts described here might result from the leaky nature of the G2 decatenation checkpoint in the cancer cells.

MCPH1 interacts *in vitro* with Plk1 and Chk1

We next investigated the potential interaction of MCPH1 with either Chk1 or Plk1 by using a pull-down approach. As MCPH1 protein includes several BRCT (breast cancer carboxyl-terminal) domains, one N-terminal and two at the C-terminus, we were also interested in analyzing the contribution of these domains to the potential interaction with Chk1 and Plk1. To accomplish this, we employed two different GFP-tagged MCPH1 constructs, one encoding full MCPH1 protein and one encoding a truncated version lacking the two C-terminal BRCT domains (see Fig. 6E). HEK293 cells were transfected with the GFP-tagged constructs, which were next purified and immunoprecipitated from cells before incubation with cells extracts containing Myc-tagged construct encoding either full Chk1 or Plk1. The potential interaction between the proteins was finally investigated by western blot using anti-GFP and anti-Myc antibodies. As presented in Fig. 6F, both GFP-tagged MCPH1 constructs were able to bind Chk1, whereas a GFP-tagged control was not. These results suggest that the two C-terminal BRCT domains of MCPH1 are dispensable for the interaction with Chk1. Moreover, our data are in agreement with previous work that reported *in vitro* [38] and *in vivo* [20] interaction between MCPH1 and Chk1. Similarly, our data revealed that both GFP-tagged MCPH1 were also capable of interacting with Plk1 while the GFP-control was not (Fig. 6F). This indicates that the last two C-terminal BRCT domains are not required for the interaction of MCPH1 with Plk1. These data are the first demonstration of the *in vitro* interaction between MCPH1 and Plk1 proteins, which would take place most likely through the N-terminal BRCT domain and/or central part of MCPH1. Further experiments are required to confirm these findings *in vivo* and to delineate the interacting regions of Plk1.

Pkl1 function is required to bypass the decatenation checkpoint in cells following Chk1 inhibition

Since our data demonstrate that cells require Plk1 function to override the decatenation checkpoint, we next examined whether Plk1 inhibition restores an efficient G2 arrest in cells with Chk1 inhibited. To this end, we first employed synchronized HeLa H2B/Red1 cells treated with the same chemical inhibitors previously described. As shown in Fig. 7A, ICRF-193 was added 6 h after release from the second thymidine block, and UCN01 and BI2536 were added 2 h later. As depicted in Fig. 7B, control and MCPH1-depleted cells were not able to enter mitosis as most of the cells remained permanently arrested in G2 upon incubation with BI2536 and UCN01. However, in parallel control samples without BI2536 addition mitotic cells rapidly accumulated as expected. Depletion of MCPH1 by siRNA did not alter this observation. When the same experiment was repeated in the presence of caffeine, we obtained the same results; that is, only when BI2536 was not added were UCN01-treated cells able

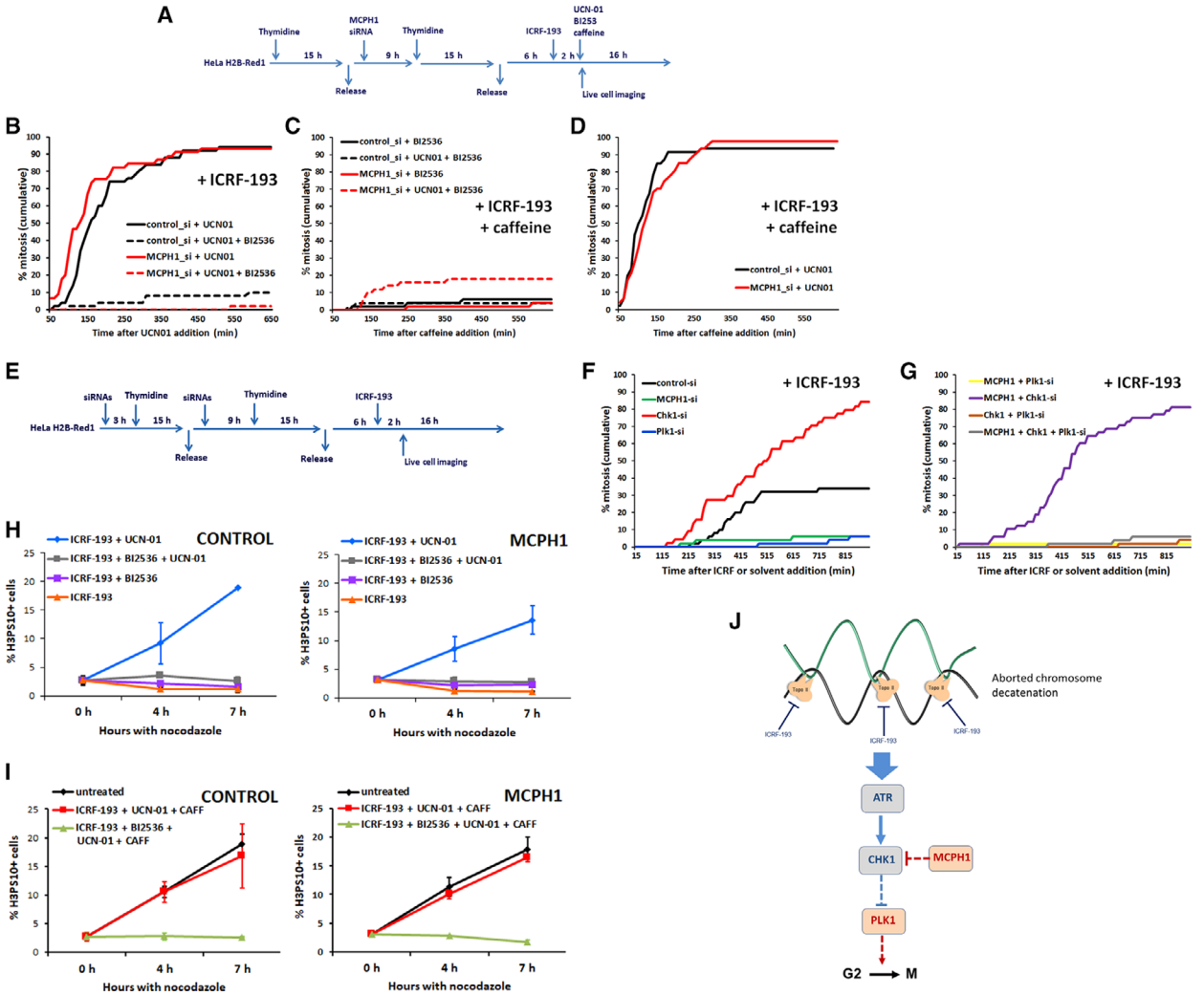

Fig. 7. Plk1 function is required to bypass the decatenation checkpoint in cells following Chk1 inhibition. (A) Description of the experimental procedure performed. HeLa H2B-Red1 cells were synchronized at the G1/S border by double thymidine block. MCPH1 depletion was achieved by transfection with siRNAs duplexes during the release from the first thymidine block. ICRF-193 (7 μM) was added 7 h after release from the second thymidine block. BI2536, UCN01, and caffeine were added 2 h later. Time-lapse phase-contrast and fluorescent images were collected immediately afterward with a Leica TCS SP5 microscope. Images were stacked and processed using IMAGEJ software. Timing data were obtained after visual inspection of mitosis onset, revealed by NEB, of 50 cells. (B–D) Cumulative frequency chart showing the timing (in minutes) of mitosis onset, revealed by NEB, of HeLa H2B-Red1 cells incubated with ICRF-193 and further treated as indicated. Time after UCN01 (B) or caffeine addition (C, D) is shown. (E) Description of the experimental procedure. HeLa H2B-Red1 was synchronized at the G1/S border by double thymidine block. Transfection with the corresponding siRNAs duplexes was performed during the incubation and release from the first thymidine block. ICRF-193 (7 μM) was added 6 h after release from the second thymidine block. Time-lapse analyses were done as explained in (A). (F, G) Cumulative frequency chart showing the timing (in minutes) of mitosis onset, revealed by NEB, of ICRF-193-treated cells transfected with the corresponding siRNAs as explained in E. Time after ICRF-193 addition is shown. (H–I) Frequency of histone H3PS10-positive cells in control and MCPH1 patient lymphoblastoid cells, determined by flow cytometry, after 4 or 7 h of incubation with nocodazole alone or in combination with the indicated inhibitors. Mean and range (bars) data from two independent experiments are presented. For each time point, pooled data for each treatment were compared independently by chi-squared test of independence to cells simultaneously treated with ICRF-193 and UCN01 (H) or to nocodazole-treated cells (I). ns, nonsignificant. (J) Model representing some components of the pathway regulating the G2 arrest induced by catalytic inhibitors of Topo II. Blue components represent factors required for triggering the G2 arrest after catalytic inhibition of Topo II, while red components are factors whose activity is indispensable for bypass of the G2 arrest.

to bypass the G2 arrest triggered by ICRF-193 (Fig. 7C,D). Again, the same dynamics were observed in cells depleted of MCPH1 function by siRNA.

To confirm these findings, we performed further analyses in HeLa H2B/Red1 cells where Plk1, Chk1, and MCPH1 proteins were depleted by siRNAs instead of inhibition with chemical inhibitors (Fig. 7E). As presented in Fig. 7G, simultaneous depletion of Plk1 combined with either Chk1 and/or MCPH1 knockdown triggered a permanent G2 arrest upon ICRF-193 incubation. However, cells retaining Plk1 function but depleted of Chk1 and MCPH1 by siRNAs bypassed the G2 arrest, in line with our previous data (Fig. 1G). Parallel control samples transfected with only one of those siRNA pairs recapitulated our previous findings (Fig. 7F). Thus, the spontaneous adaptation capacity observed for a fraction of cells upon ICRF-193 incubation was boosted by Chk1 depletion but repressed upon either Plk1 or MCPH1 depletion.

We finally determined whether similar results are obtained in lymphoblastoid cells. To address this, we analyzed the rate of mitotic entry in lymphoblastoid cells during prolonged incubation with ICRF-193, BI2536, and/or UCN01 (Fig. 7H). Our data revealed that upon triple incubation neither control nor MCPH1 patient cells enter mitosis during the time course of our experiment. The dynamics observed were similar to those from cells incubated with ICRF-193 and BI2536 or single incubated with ICRF-193. Furthermore, caffeine addition did not force cells into mitosis while incubated with ICRF-193, BI2536, and UCN01 (Fig. 7I). However, when Plk1 function was not inhibited with BI2536, the G2 arrest was efficiently bypassed in cells treated under the same conditions (Fig. 7I). From these combined results, it can be concluded that both caffeine- and Chk1-block-mediated bypass of an ICRF-193-induced G2 checkpoint requires Plk1 activity. These results clearly indicate that Plk1 is likely to act downstream of Chk1 and MCPH1 in the pathway that triggers bypass of the decatenation checkpoint arrest (Fig. 7J). In this context, MCPH1 function appears critical to allow checkpoint adaptation by counteracting Chk1-mediated inactivation of Plk1.

Discussion

The G2 decatenation checkpoint delays entry into mitosis if chromosomes are insufficiently decatenated by Topo II [10,15]. Previous studies have provided evidence of the leaky nature of this G2 arrest compared with other G2 checkpoints, such as the DNA damage response triggered by DSBs [9]. Consequently, upon Topo II inhibition many cells have the capacity to resume cell cycle progression following a transient arrest, and perform mitosis with catenated chromosomes. In some types of cancer cells, this checkpoint is extremely attenuated or is entirely defective [18,39-41]. Therefore, adaptation to the Topo II-dependent G2 arrest is a cellular process with potential implications for genome instability and tumor initiation or formation. However, the mechanism of adaptation remains poorly understood. In a previous study, we have shown that MCPH1, a gene mutated in primary microcephaly syndrome, is essential to confer adaptation to the decatenation checkpoint in human cells [9]. Here, we have demonstrated that the incapacity to bypass the decatenation G2 arrest observed in MCPH1-depleted cells is not a consequence of defective recovery, or exit, from this checkpoint since these cells were able to resume cell cycle progression after release from prolonged incubation with ICRF-193. This was important to establish because less attention has been paid to the distinction between adaptation versus checkpoint recovery processes in many studies. Thus, careful validation of the genes identified as specific regulators of checkpoint adaptation is required since both adaptation and recovery processes share some effectors that might produce identical cell cycle dynamics when depleted [42].

Here, we provide biological evidence supporting opposite roles for Chk1 and Plk1 in the pathway regulating mitotic entry upon Topo II inhibition. As the decatenation checkpoint relies entirely on ATR signaling [13], it is not difficult at first to envisage an active role for Chk1 in this pathway. However, previous studies presented contradictory results concerning the role of Chk1 in this checkpoint [13,19]. Our present results clearly confirm that Chk1 function is required to sustain the G2 arrest triggered by ICRF-193 in human cells. This requirement is in line with previous studies, which have shown that chicken bursal lymphoma cell line (DT40) $Chk1^{-/-}$ cells harbor a defective decatenation checkpoint [19]. Furthermore, the incapacity of MCPH1-depleted cells to bypass the decatenation checkpoint arrest was restored if Chk1 function was simultaneously compromised. Taken together, our data indicate that MCPH1 confers cellular adaptation to the decatenation checkpoint by counteracting the inhibitory activity of Chk1 triggered upon Topo II inhibition.

The interplay between MCPH1 and Chk1 has been previously described in other contexts. Thus, MCPH1 regulates centrosomal Chk1 function during unperturbed cell cycle progression [20]. Moreover, MCPH1

function appears critical to restrict the levels of active Chk1 during the cell response to ionizing radiation (IR) [21]. This negative effect could explain the lengthened recovery from the G2 DNA damage checkpoint arrest previously described for MCPH1 patient cells [43,44]. Importantly, our previous analyses have shown that MCPH1 function is not required to bypass the DNA damage checkpoint, which is bypassed by caffeine in MCPH1-depleted cells with similar kinetics to control cells [9]. Therefore, the requirement of MCPH1 to bypass the Chk1-related G2 arrest is related to specific unknown signals that arise upon catalytic inhibition of Topo II by ICRF-193. These data are apparently difficult to reconcile with the defective response described previously in MCPH1 patient cells upon replication stress or UV radiation, both DNA insults that rely on ATR signaling [38]. According to the authors, MCPH1 is required downstream of Chk1 for triggering an efficient ATR-related checkpoint arrest in response to those insults. However, our analyses demonstrated that MCPH1 does not contribute to sustain a G2 arrest in response to catalytic inhibition of Topo II, which relies on ATR signaling, but is required to confer the capacity to bypass the checkpoint [9]. Further analyses are necessary to better understand the contribution of MCPH1 within pathways that rely on ATR but respond to different types of genotoxic stress.

Previous studies have shown that ICRF-193-treated cells display a significant, albeit-not complete inhibition of Plk1 activity [27]. Moreover, overexpression of a constitutively active Plk1 variant abolished the decatenation checkpoint response [14,27]. These data demonstrate that ICRF-193-meditated G2 arrest requires inhibition of Plk1 activity, which prompted us to investigate whether Plk1 activity is essential in the opposite context, that is, during checkpoint adaptation. Our current analyses confirmed that Plk1 function is required to bypass the G2 arrest triggered in response to Topo II catalytic inhibition. Furthermore, our data provide evidence that Plk1 likely acts downstream of MCPH1 and Chk1 in this pathway (Fig. 7J). Interestingly, Plk1 is also essential during cellular adaptation to the DNA damage checkpoint that responds to DSBs [5,7,31]. Furthermore, Chk1 activity is also required in human cells to sustain the IR-induced checkpoint [7,42]. Upon permanent DNA damage, both Plk1 and Chk1 control checkpoint adaptation in part through independent signaling pathways which converge on a common possible target, Cyclin B/Cdk1 [42]. Therefore, while Plk1 is commonly required to bypass both the DNA damage and the decatenation checkpoint, other regulators specific to each checkpoint pathway must exist. This is the case for MCPH1, which might act upstream of Plk1 by counteracting Chk1 activity in order to confer cellular adaptation in response to alterations in the topology of the DNA (Fig. 7J). However, MCPH1 does not contribute similarly in response to UV- or IR-induced damage [38]. These results led us to hypothesize the existence of common signals upon the multiple pathways that regulate cellular adaptation to a G2 arrest, as it is the case for Plk1, which are further modulated by regulators that respond specifically to each type of genotoxic stress, as MCPH1 does upon catalytic inhibition of Topo II.

Our study adds novel insight into the genetic requirements that provide cells with the capacity to bypass the G2 arrest triggered by Topo II inhibition. A recent study has identified SMC5/6 as a novel regulator of this checkpoint arrest by using a genome-wide RNAi screen [12]. This study confirmed the roles of ATR and Topo II in this checkpoint but failed to recapitulate an impact on it upon RNAi depletion of other identified players such as Brca1, WRN, MDC, or Chk1. This discrepancy was explained by the use of transformed cells such as HeLa or DT40 in those previous studies, in which compromised redundant pathways leave these cell lines critically dependent on such regulators. In our study, Chk1 function was required to sustain the G2 Topo II checkpoint arrest in both transformed HeLa and nontransformed lymphoblastoid cells. According to our data, other possibilities might be considered to explain the discrepancies concerning Chk1, such as insufficient knockdown or differences in methodology. Interestingly, no checkpoint arrest was observed upon Chk1 depletion in ICRF-193-treated human cells containing mutated (HeLa) or wild-type p53 (lymphoblasts). Previous studies demonstrated that adaptation to irradiation in human cells does not depend on p53 [7]. In line with this, our evidence suggests that bypass of G2 decatenation checkpoint also does not require p53 deficiency.

Checkpoint adaptation is considered a potential contributor to tumorigenesis as it increases the risk of genome instability during successive cell divisions [42]. Related to this, the attenuated status of the G2 decatenation checkpoint described in different tumor cells could have favored oncogenesis by inducing chromosome instability phenotypes [18]. The requirement of MCPH1 for orchestrating cellular adaptation to the decatenation checkpoint might be of importance to better understand recent evidence implicating MCPH1 in tumorigenesis [11]. On the other hand, an additional scenario to be considered is the potential association of decatenation checkpoint bypass with the process of

mitotic cell death. This process has been described in some cells upon adaptation to irradiation and is considered a fail-safe pathway that allows cell death at later stages for those cells unable to enter in apoptosis during a G2 arrest [7,45]. Given this evidence, it will be of interest to investigate whether a similar process is prompted in cells capable—or incapable—of bypassing the G2 decatenation checkpoint arrest.

Material and methods

Cell cultures and treatments

We have used standard and modified (H2B-Red1 tagged) HeLa cell lines. Furthermore, we employed lymphoblast cell lines (LCLs, nontransformed EBV immortalized) from one MCPH1 patient (S25X mutation) and one healthy control subject [22,46]. For pull-down analyses, we employed HEK293 cells. HeLa and HEK293 cells were grown following standard conditions using Dulbecco's modified Eagle's medium (DMEM) medium supplemented with 10% of FBS. LCLs were grown under usual conditions in RPMI medium supplemented with 15% FBS.

For RNAi treatments, cells were transfected with 120 nM siRNA duplexes using Lipofectamine (Invitrogen, Thermo Fisher Scientific, Waltham, MA USA) at 50% confluence. OptiMEM medium (Invitrogen) was used for cell transfection. The MCPH1_siRNA duplexes used were purchased from Qiagen (Germantown, MD, USA) and are based on previous studies [9,47,48]. For Plk1, we employed siRNA duplexes based on a previous study [49] that were purchased from Qiagen. Alternatively, we also employed commercial siRNA duplexes against Plk1 to confirm our results (Ambion, Thermo Fisher Scientific, Waltham, MA, USA). The siRNA employed to deplete Chk1 was commercial (Santa Cruz Biotechnology, Dallas, TX, USA). As a control, we used negative scramble siRNA duplexes (Thermo Fisher Scientific). Synchronization of cells at G1/S was achieved by a double thymidine block protocol. The inhibitors employed were nocodazole (final concentration 1.5 μM), ICRF-193 (final concentration 7 μM), caffeine (final concentration 2 mM), UCN01 (final concentration 300 nM), BI2536 (final concentration 1 μM), CHIR-124 (Selleckchem, Houston, TX, USA; final concentration 100 nM), and MK1775 (Selleckchem, final concentration 300 nM). Untreated control cells were in all cases incubated with a similar volume of solvent. All reagents were purchased from Sigma (St. Louis, MO, USA) unless noted otherwise.

Live-cell microscopy

The procedure was similar to the described in [9,47]. Cells were plated onto 35-mm tissue culture dishes fitted with glass coverslips (Cultureware; MatTek, Ashland, MA, USA). siRNA transfection and cell synchrony were performed as described in the results section, except that upon release from the second thymidine the standard medium containing the thymidine was exchanged for DMEM without phenol red, supplemented with 10% FBS, penicillin/streptomycin, and 200 mM Trolox (Calbiochem, San Diego, CA, USA). The dishes were transferred to a microscope humidified stage incubator containing 5% CO_2 at 37 °C. Cells were filmed with three to five z sections using a Leica TCS SP5 microscope (Leica Microsystems, Wetzlar, Germany). Images were stacked and processed using IMAGEJ (National Institutes of Health, Bethesda, MD, USA) software. Timing data were obtained after visual inspection of a minimum of 50 cells. Statistical comparisons were done using STATGRAPHICS software (Statgraphics Technologies, The Plains, VA, USA).

Flow cytometry

Flow cytometry analyses were done using lymphoblast cell cultures in log-phase. Approximately one million cells were recovered, washed in PBS, and fixed in ice-cold Ethanol 70 overnight. Phospho-histone H3-positive cells were detected with a rabbit anti-histone H3PS10 antibody (Abcam, Cambridge, MA, USA) with a dilution of 1/250, and a donkey anti-mouse IgG FITC-conjugated secondary antibody (Santa Cruz). Propidium iodide was used as a counterstain for DNA content. Fluorescence detection was performed using an analytical flow cytometer (LSR Fortessa; BD Biosciencie, San Jose, CA, USA) equipped with BD FACSDIVA™ software for data acquisition. Quantitative cell cycle analysis was done with FLOWING Software v.2.5.1 as explained in [9,47].

Cytogenetic analyses

Cytogenetic preparations following standard protocols were obtained in parallel from the same log-phase cell cultures analyzed by flow cytometry. Chromosome preparations were fixed using Carnoy's solution (methanol/glacial acetic acid, 3 : 1), stained with Giemsa (10 %), and finally visualized by bright-field microscopy. Microscopy images were captured with a CCD camera (Olympus DP70, Olympus, Tokyo, Japan) coupled to a microscope (Olympus BX51) and finally managed with IMAGEJ software.

Immunoblot and pull-down analyses

For immunoblot analyses of siRNA knockdown experiments, approximately 1×10^5 cells were suspended in 100 μL lysis buffer, sonicated, and boiled for 2 min. Proteins were resolved by SDS/PAGE and transferred to Hybond-P PVDF membranes (Amersham, Little Chalfont, UK). The membrane was blocked with 2.5% (w/v) dry milk in TBST (20 mM Tris/HCl [pH 7.5], 150 mM NaCl, 0.05% Tween-20). Incubation with primary

antibodies was performed in TBST containing 1% BSA and 0.05% sodium azide overnight at 4 °C. Blots were developed by enhanced chemiluminescence detection system (Amersham). Primary antibodies used were anti-total Chk1 (sc-8408; Santa Cruz), anti-Plk1 (MA1-848; Thermo Fisher), anti-MCPH1 (11962-1-AP; Proteintech, Manchester, UK), and anti-alpha tubulin (T5168; Sigma) as loading control.

For pull-down analyses, we employed plasmids encoding full MCPH1 protein or a MCPH1 fragment lacking the two C-terminal BRCT domains. These plasmids were tagged with an N-terminal GFP tag and were kindly provided by P. A. Jowsey (University of Newcastle, UK). We also employed a plasmid encoding full Chk1 tagged with an N-terminal Myc tag, kindly provided by C. Morrison (University of Galway, Ireland), and a plasmid-encoding full Plk1 tagged with an N-terminal Myc tag, kindly provided by G. deCárcer (IIBM—CSIC, Spain). To evaluate the potential *in vitro* interaction of GFP-MCPH1 constructs with myc-Chk1 or myc-Plk1, we used the following strategy. First, HEK293 cells were transfected with GFP-MCPH1 constructs or GFP alone using a standard calcium phosphate protocol. Next, after 48 h of transfection cells extracts were obtained after cold PBS washing with NETN lysis buffer (50 mM Tris pH 7.6, 150 mM NaCl, 1 mM EDTA, and 1% NP-40), including protease and phosphatase inhibitor (MS-SAFE cocktail, MilliporeSigma, Burlington, MA, USA). Cell lysates were incubated with GFP-Trap (Chromotek, Planegg-Martinsried, Germany) to purify GFP-tagged proteins for 2 h at 4 °C, and then, two washes with TBST buffer (50 mM Tris pH 7.6, 150 mM NaCl, and 0.2% Tween-20) and one further wash with NETN buffer were applied. Fifteen percent of the original cell lysate was used as negative binding control (input), following the same procedure but without incubation with the GFP-Trap reagent. GFP-trap beads containing immobilized GFP-MCPH1 and GFP alone were incubated with cell extracts obtained from HEK293 cells transfected with either myc-Chk1 or myc-Plk1 plasmids in which 15% of the cell lysate was used as input. After incubation for 3 h at 4 °C, the beads were washed three times in TBST buffer and suspended in 2xLDS sample buffer (Thermo Fisher Scientific) containing 5% 2-ME and heated to 70 °C for 10 min. Finally, all the samples were analyzed by immunoblot as explained above using the following primary antibodies: rat monoclonal anti-GFP (AB-ID255; Chromotek) and mouse anti-myc (kindly provided by Cristina Cardoso and described in [50]).

Ethic statement

This study was approved by 'Comisión de Etica', Vicerrectorado de Investigación, Universidad de Jaén, Spain, under the reference number OMGsABs-385.

Acknowledgments

The authors express their gratitude to: H. Neitzel (Institute of Medical and Human Genetics, Charité—Universitaetsmedizin Berlin) for providing the lymphoblast cell lines used in this study; Nieves de la Casa (CICT, Universidad de Jaén, Spain) for technical assistance; Paul A. Jowsey (University of Newcastle, UK) for providing MCPH1 plasmids; Ciaran Morrison (University of Galway, Ireland), for providing Chk1 plasmid; Gillermo deCárcer (IIBm-CSIC, Spain), for providing Plk1 plasmid; and Ryoko Kuriyama (University of Minnesota, USA) for helpful discussions. We kindly appreciate the technical support of Cristina Cardoso (University of Darmstadt, Germany) during the revision procedure. Technical and human support provided by CICT of Universidad de Jaén (UJA, MINECO, Junta de Andalucía, FEDER) is gratefully acknowledged. This work was supported by Junta de Andalucía (Funding program 'Ayudas a grupos de investigación', reference RMN-924) and Consejería de Salud, Junta de Andalucía (Grant number PI-0110-2017). Research in the laboratory of D. Clarke was financially supported by NIH grants R01GM112793 and R01GM130858. M. Arroyo PhD was granted by University of Jaén (Spain) and was provided with traveling grants to perform short-term stays at the University of Minnesota by EMBO and 'Escuela de Doctorado' (University of Jaén, Spain), respectively.

Author contribution

MA and JAM designed the experiments. MA, JC, FDH, and JAM performed the experiments. MA, AC, AS, DJC, and JAM analyzed the results. JAM and DJC wrote the main manuscript text. All authors reviewed the manuscript.

Conflict of interest

The funders had no role in study design, data collection and analysis, decision to publish, or preparation of the manuscript. The corresponding author, on behalf of all authors of the paper, declares no conflict of interest.

References

1 Langerak P & Russell P (2011) Regulatory networks integrating cell cycle control with DNA damage checkpoints and double-strand break repair. *Philos Trans R Soc B Biol Sci* **366**, 3562–3571.

2 Jackson SP & Bartek J (2010) The DNA-damage response in human biology and disease. *Nature* **461**, 1071–1078.
3 Bartek J & Lukas J (2007) DNA damage checkpoints: from initiation to recovery or adaptation. *Curr Opin Cell Biol* **19**, 238–245.
4 Sandell LL & Zakian VA (1993) Loss of a yeast telomere: arrest, recovery, and chromosome loss. *Cell* **75**, 729–739.
5 Toczyski DP, Galgoczy DJ & Hartwell LH (1997) CDC5 and CKII control adaptation to the yeast DNA damage checkpoint. *Cell* **90**, 1097–1106.
6 Yoo HY, Kumagai A, Shevchenko A, Shevchenko A & Dunphy WG (2004) Adaptation of a DNA replication checkpoint response depends upon inactivation of Claspin by the Polo-like kinase. *Cell* **117**, 575–588.
7 Syljuasen RG, Jensen S, Bartek J & Lukas J (2006) Adaptation to the ionizing radiation-induced G2 checkpoint occurs in human cells and depends on checkpoint kinase 1 and polo-like kinase 1 kinases. *Cancer Res* **66**, 10253–10257.
8 Serrano D & D'Amours D (2014) When genome integrity and cell cycle decisions collide: roles of polo kinases in cellular adaptation to DNA damage. *Syst Synth Biol* **8**, 195–203.
9 Arroyo M, Kuriyama R, Guerrero I, Keifenheim D, Cañuelo A, Calahorra J, Sánchez A, Clarke DJ & Marchal JA (2019) MCPH1 is essential for cellular adaptation to the G2-phase decatenation checkpoint. *FASEB J* **33**, 8363–8374.
10 Damelin M & Bestor TH (2007) The decatenation checkpoint. *Br J Cancer* **96**, 201–205.
11 Venkatesh T & Suresh PS (2014) Emerging roles of MCPH1: expedition from primary microcephaly to cancer. *Eur J Cell Biol* **93**, 98–105.
12 Deiss K, Lockwood N, Howell M, Segeren HA, Saunders RE, Chakravarty P, Soliman TN, Martini S, Rocha N, Semple R *et al.* (2018) A genome-wide RNAi screen identifies the SMC5/6 complex as a non-redundant regulator of a Topo2a-dependent G2 arrest. *Nucleic Acids Res* **47**, 2906–2921, 1–16.
13 Deming PB, Cistulli CA, Zhao H, Graves PR, Piwnica-Worms H, Paules RS, Downes CS & Kaufmann WK (2001) The human decatenation checkpoint. *Proc Natl Acad Sci USA* **98**, 12044–12049.
14 Luo K, Yuan Jian, Chen J & Lou Zhenkun (2009) NIH public access. *Nat Cell Biol* **19**, 389–399.
15 Stephen Downes C, Clarke DJ, Mullinger AM, Giménez-Abián JF, Creighton AM & Johson RT (1993) A topoisomerase II-dependent G2 cycle checkpoint in mammalian cells/. *Nature* **372**, 467–470.
16 Franchitto A, Oshima J & Pichierri P (2003) The G2-phase decatenation checkpoint is defective in Werner syndrome cells. *Cancer Res* **63**, 3289–3295.
17 Lou Z, Minter-Dykhouse K & Chen J (2005) BRCA1 participates in DNA decatenation. *Nat Struct Mol Biol* **12**, 589–593.
18 Nakagawa T, Hayashita Y, Maeno K, Masuda A, Sugito N, Osada H, Yanagisawa K, Ebi H, Shimokata K & Takahashi T (2004) Identification of decatenation G2checkpoint impairment independently of DNA damage G2checkpoint in human lung cancer cell lines. *Cancer Res* **64**, 4826–4832.
19 Robinson HMR, Bratlie-Thoresen S, Brown R & Gillespie DAF (2007) Chk1 is required for G2/M checkpoint response induced by the catalytic topoisomerase II inhibitor ICRF-193. *Cell Cycle* **6**, 1265–1267.
20 Tibelius A, Marhold J, Zentgraf H, Heilig CE, Neitzel H, Ducommun B, Rauch A, Ho AD, Bartek J & Krämer A (2009) Microcephalin and pericentrin regulate mitotic entry via centrosome-associated Chk1. *J Cell Biol* **185**, 1149–1157.
21 Antonczak AK, Mullee LI, Wang Y, Comartin D, Inoue T, Pelletier L & Morrison CG (2016) Opposing effects of pericentrin and microcephalin on the pericentriolar material regulate Chk1 activation in the DNA damage response. *Oncogene* **35**, 2003–2010.
22 Neitzel H, Neumann LM, Schindler D, Wirges A, Tönnies H, Trimborn M, Krebsova A, Richter R & Sperling K (2002) Premature chromosome condensation in humans associated with microcephaly and mental retardation: a novel autosomal recessive condition. *Am J Hum Genet* **70**, 1015–1022.
23 Arroyo M, Trimborn M, Sánchez A, Hirano T, Neitzel H & Marchal JA (2015) Chromosome structure deficiencies in MCPH1 syndrome. *Chromosoma* **124**, 491–501.
24 Graves PR, Yu L, Schwarz JK, Gales J, Sausville EA, O'Connor PM & Piwnica-Worms H (2000) The Chk1 protein kinase and the Cdc25C regulatory pathways are targets of the anticancer agent UCN-01. *J Biol Chem* **275**, 5600–5605.
25 Bower JJ, Karaca GF, Zhou Y, Simpson DA, Cordeiro-Stone M & Kaufmann WK (2010) Topoisomerase IIalpha maintains genomic stability through decatenation G(2) checkpoint signaling.. *Oncogene* **29**, 4787–4799.
26 Giménez-Abián JF, Clarke DJ, Devlin J, Giménez-Abián MI, De La Torre C, Johnson RT, Mullinger AM & Downes CS (2000) Premitotic chromosome individualization in mammalian cells depends on topoisomerase II activity. *Chromosoma* **109**, 235–244.
27 Deming PB, Flores KG, Stephen Downes C, Paules RS & Kaufmann WK (2002) ATR enforces the topoisomerase II-dependent G 2 checkpoint through inhibition of Plk1 kinase. *J Biol Chem* **277**, 36832–36838.
28 Steegmaier M, Hoffmann M, Baum A, Lénárt P, Petronczki M, Krššák M, Gürtler U, Garin-Chesa P,

Lieb S, Quant J *et al.* (2007) BI 2536, a potent and selective inhibitor of polo-like kinase 1, inhibits tumor growth *in vivo*. *Curr Biol* **17**, 316–322.
29 Lénárt P, Petronczki M, Steegmaier M, Di Fiore B, Lipp JJ, Hoffmann M, Rettig WJ, Kraut N & Peters JM (2007) The Small-molecule inhibitor BI 2536 reveals novel insights into mitotic roles of polo-like kinase 1. *Curr Biol* **17**, 304–315.
30 Aspinall CF, Zheleva D, Tighe A & Taylor SS (2015) Mitotic entry: Non-genetic heterogeneity exposes the requirement for Plk1. *Oncotarget* **6**, 36472–36488.
31 Van Vugt MATM, Brás A & Medema RH (2004) Polo-like kinase-1 controls recovery from a G2 DNA damage-induced arrest in mammalian cells. *Mol Cell* **15**, 799–811.
32 Petronczki M, Lénárt P & Peters JM (2008) Polo on the rise-from mitotic entry to cytokinesis with Plk1. *Dev Cell* **14**, 646–659.
33 Lindqvist A, Rodríguez-Bravo V & Medema RH (2009) The decision to enter mitosis: feedback and redundancy in the mitotic entry network. *J Cell Biol* **185**, 193–202.
34 Hirai H, Iwasawa Y, Okada M, Arai T, Nishibata T, Kobayashi M, Kimura T, Kaneko N, Ohtani J, Yamanaka K *et al.* (2009) Small-molecule inhibition of Wee1 kinase by MK-1775 selectively sensitizes p53-deficient tumor cells to DNA-damaging agents. *Mol Cancer Ther* **8**, 2992–3000.
35 Potapova TA, Sivakumar S, Gorbsky GJ, Flynn JN & Li R (2011) Mitotic progression becomes irreversible in prometaphase and collapses when Wee1 and Cdc25 are inhibited. *Mol Biol Cell* **22**, 1191–1206.
36 Watanabe N, Arai H, Nishihara Y, Taniguchi M, Watanabe N, Hunter T & Osada H (2004) M-phase kinases induce phospho-dependent ubiquitination of somatic Wee1 by SCFβ-TrCP. *Proc Natl Acad Sci USA* **101**, 4419–4424.
37 Watanabe N, Arai H, Iwasaki J, Shiina M, Ogata K, Hunter T & Osada H (2005) destabilizes somatic Wee1 via multiple pathways. *Proc Natl Acad Sci USA* **102**, 11663–11668.
38 Alderton GK, Galbiati L, Griffith E, Surinya KH, Neitzel H, Jackson AP, Jeggo PA & O'Driscoll M (2006) Regulation of mitotic entry by microcephalin and its overlap with ATR signalling. *Nat Cell Biol* **8**, 725–733.
39 Brooks K, Chia KM, Spoerri L, Mukhopadhyay P, Wigan M, Stark M, Pavey S & Gabrielli B (2014) Defective decatenation checkpoint function is a common feature of melanoma. *J Invest Dermatol* **134**, 150–158.
40 Singh N, Wiltshire TD, Thompson JR, Mer G & Couch FJ (2012) Molecular basis for the association of microcephalin (MCPH1) protein with the cell division cycle protein 27 (Cdc27) subunit of the anaphase-promoting complex. *J Biol Chem* **287**, 2854–2862.
41 Bower JJ, Vance LD, Psioda M, Smith-Roe SL, Simpson DA, Ibrahim JG & Hoadley KA, Perou CM & Kaufmann WK (2017) Patterns of cell cycle checkpoint deregulation associated with intrinsic molecular subtypes of human breast cancer cells. *NPJ Breast Cancer* **3**, 1–9.
42 Syljuåsen RG (2007) Checkpoint adaptation in human cells. *Oncogene* **26**, 5833–5839.
43 Brown JAL, Bourke E, Liptrot C, Dockery P & Morrison CG (2010) MCPH1/BRIT1 limits ionizing radiation-induced centrosome amplification. *Oncogene* **29**, 5537–5544.
44 Gavvovidis I, Pöhlmann C, Marchal JA, Stumm M, Yamashita D, Hirano T, Schindler D, Neitzel H & Trimborn M (2010) MCPH1 patient cells exhibit delayed release from DNA damage-induced G2/M checkpoint arrest. *Cell Cycle* **9**, 4893–4899.
45 Swift LH & Golsteyn RM (2014) Genotoxic anti-cancer agents and their relationship to DNA damage, mitosis, and checkpoint adaptation in proliferating cancer cells. *Int J Mol Sci* **15**, 3403–3431.
46 Trimborn M, Bell SM, Felix C, Rashid Y, Jafri H, Griffiths PD, Neumann LM, Krebs A, Reis A, Sperling K *et al.* (2004) Mutations in microcephalin cause aberrant regulation of chromosome condensation. *Am J Hum Genet* **75**, 261–266.
47 Arroyo M, Kuriyama R, Trimborn M, Keifenheim D, Cañuelo A, Sánchez A, Clarke DJ & Marchal JA (2017) MCPH1, mutated in primary microcephaly, is required for efficient chromosome alignment during mitosis. *Sci Rep* **7**, 13019.
48 Gavvovidis I, Rost I, Trimborn M, Kaiser FJ, Purps J, Wiek C, Hanenberg H, Neitzel H & Schindler D (2012) A novel MCPH1 isoform complements the defective chromosome condensation of human MCPH1-deficient cells. *PLoS ONE* **7**, 1–12.
49 Gimenez-Abian JF, Sumara I, Hirota T, Hauf S, Gerlich D, de la Torre C, Ellenberg J & Peters JM (2004) regulation of sister chromatid cohesion between chromosome arms. *Curr Biol* **14**, 1187–1193.
50 Evan GI, Lewis GK, Ramsay G & Bishop JM (1985) Isolation of monoclonal antibodies specific for human c-myc proto-oncogene product. *Mol Cell Biol* **5**, 3610–3616.